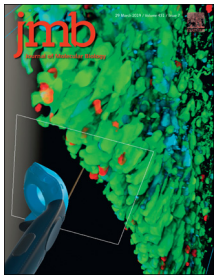

Unique Unfoldase/Aggregase Activity of a Molecular Chaperone Hsp33 in its Holding-Inactive State

Ku-Sung Jo [1,†], Ji-Hun Kim [2], Kyoung-Seok Ryu [3], Joo-Seong Kang [1], Chae-Yeon Wang [1], Yoo-Sup Lee [1,4], Min-Duk Seo [4], Young-Ho Lee [3] and Hyung-Sik Won [1]

*1 - **Department of Biotechnology,** Research Institute (RIBHS) and College of Biomedical & Health Science, Konkuk University, Chungju, Chungbuk 27478, Republic of Korea*
*2 - **College of Pharmacy,** Chungbuk National University, Cheongju, Chungbuk 28160, Republic of Korea*
*3 - **Protein Structure Group,** Korea Basic Science Institute, Ochang, Chungbuk 28199, Republic of Korea*
*4 - **College of Pharmacy and Department of Molecular Science and Technology,** Ajou University, Suwon, Gyeonggi 16499, Republic of Korea*

***Correspondence to Hyung-Sik Won:** Department of Biotechnology, Konkuk University, Chungwon-daero 268, Chungju, Chungbuk 380-701, Republic of Korea. wonhs@kku.ac.kr*
https://doi.org/10.1016/j.jmb.2019.02.022
Edited by J. Buchner

Abstract

The various chaperone activities of heat shock proteins contribute to ensuring cellular proteostasis. Here, we demonstrate the non-canonical unfoldase activity as an inherent functionality of the prokaryotic molecular chaperone, Hsp33. Hsp33 was originally identified as a holding chaperone that is post-translationally activated by oxidation. However, in this study, we verified that the holding-inactive reduced form of Hsp33 (^{R}Hsp33) strongly bound to the translational elongation factor, EF-Tu. This interaction was critically mediated by the redox-switch domain of ^{R}Hsp33 and the guanine nucleotide-binding domain of EF-Tu. The bound ^{R}Hsp33, without undergoing any conformational change, catalyzed the EF-Tu aggregation by evoking the aberrant folding of EF-Tu to expose hydrophobic surfaces. Consequently, the oligomers/aggregates of EF-Tu, but not its functional monomeric form, were highly susceptible to proteolytic degradation by Lon protease. These findings present a unique example of an ATP-independent molecular chaperone with distinctive dual functions—as an unfoldase/aggregase and as a holding chaperone—depending on the redox status. It is also suggested that the unusual unfoldase/aggregase activity of ^{R}Hsp33 can contribute to cellular proteostasis by dysregulating EF-Tu under heat-stressed conditions.

Introduction

Molecular chaperones, such as heat shock proteins (Hsps), are widely recognized as vital mediators of cellular protein conformation and protein turnover (i.e., the balance between protein synthesis and protein degradation) [1]. Owing to the flexible and labile nature of protein structures, a complex and dynamic network of molecular chaperones constituting an elaborate machinery of protein quality control protects the cellular proteome under both normal and stressed conditions [2–4]. In particular, as misfolded and/or denatured proteins are prone to aberrant behavior, such as formation of irreversible aggregates that are deleterious to cells, molecular chaperones assist in the correct *de novo* folding and refolding of proteins, and function to prevent proteins from aberrant folding and aggregation [5,6]. In some cases, molecular chaperones are also associated with the timely removal of irreversibly misfolded proteins. As such, molecular chaperones play central roles in ensuring cellular proteostasis (i.e., proteome homeostasis) that also requires a regulated process of protein turnover [7–9]. Therefore, various molecular activities including foldase, refoldase, unfoldase, holding, disaggregase, translocase, and targetase activities are associated with chaperone functions [10]. Among these, the unfoldase activity of molecular chaperones, which is

somewhat in conflict with its overall function in conformational maintenance, generally catalyzes the unfolding of stable misfolded proteins to convert them into natively refoldable or readily cleavable states. This unfoldase activity is therefore directly linked to other inherent chaperone activities, such as the sequential reaction for disaggregation–unfolding–refolding of stable soluble aggregates [10,11] or in the case of AAA+ proteases that unfold misfolded substrate proteins for subsequent degradation [12,13]. In both cases, those molecular chaperones with the transient unfoldase reactions essentially consume ATP for their ultimate chaperone functions. Here, we report a novel type of unfoldase activity identified in the ATP-independent molecular chaperone, Hsp33, which induces irreversible aggregation of the substrate protein.

The prokaryotic molecular chaperone Hsp33 was originally discovered as a heat-inducible but post-translationally activated chaperone [4,14]. The protein requires dual stressors of heat and oxidation [15] or a severe acute oxidative stress signal [16] to display its ATP-independent holding activity, which results in its binding to the unfolding intermediates of client proteins to prevent their ultimate irreversible denaturation. The reduced form of Hsp33 (^{R}Hsp33), which is inactive in terms of the holding chaperone function, has a unique fold of the redox-switch domain (RSD; residues 232–294) that binds a zinc ion *via* four conserved cysteines (C232, C234, C265, and C268) [17]. Thus, under oxidative heat or kinetically fast oxidative conditions, the functionally active, oxidized form of Hsp33 (^{O}Hsp33) is formed *via* release of zinc due to the formation of disulfide bonds (C232–C234 and C265–C268 linkages) between the cysteines. In this holding-active conformation, the middle linker domain (MLD; residues 179–231) and the RSD become disordered to provide client-binding sites [18,19]. However, mild oxidation of ^{R}Hsp33 at a non-elevated temperature predominantly produces a half-oxidized form of the protein (^{hO}Hsp33) with only one disulfide bond (C265-C268) in which the RSD is unfolded but the MLD remains folded, and the protein shows little to no activity [15,20]. Subsequent studies revealed that unfolding of the RSD is not the structural determinant for functional activation of Hsp33, although it serves as a redox-sensing module [21,22]. This observation, together with the facts that Hsp33 is expressed at a basal level even under non-stressed conditions [4] and heat shock itself does not provide an adequate stimulus for the thermally overexpressed Hsp33 to achieve its holding chaperone activity, led us to speculate that ^{R}Hsp33 may possess its own specific functionality *via* the unique fold of the RSD. In this regard, we considered the findings of controversial reports [23–25] investigating the effects of Hsp33 on elongation factor thermal-unstable (EF-Tu), a translational GTPase playing an essential role in translation elongation by delivering aminoacyl-tRNA to the ribosomal A site [26,27]. For example, Wholey and Jakob [23] observed that Hsp33 protected EF-Tu against oxidative degradation in *Vibrio cholerae*, whereas Bruel *et al*. [24] demonstrated that Hsp33 overexpression targeted EF-Tu for degradation in an *Escherichia coli* strain lacking trigger factor and DnaK. However, in both cases, the molecular interaction of Hsp33 with EF-Tu was not investigated at the molecular structural level.

In this context, the aim of the present study was to uncover the novel functionality of Hsp33 and to underpin the structural basis of this functionality. In addition to verifying the direct molecular interaction, we aimed to identify which of the multiple conformations of Hsp33 (^{R}Hsp33, ^{hO}Hsp33, and ^{O}Hsp33) is primarily responsible for the EF-Tu interaction, in order to determine whether this conformation protects or destabilizes EF-Tu, and to identify the structural and functional consequences of the interaction. Overall, the results demonstrated that ^{R}Hsp33 specifically displays unique unfoldase/aggregase activity against EF-Tu, which can have several biological implications, including the possible involvement of Hsp33 in both the protein quality control machinery and the regulatory system of protein turnover.

Results

Oligomerizing and aggregating tendency of EF-Tu

Initial preparation of recombinant EF-Tu using no particular additives resulted in a heterogeneous mixture of the protein, indicative of various oligomeric states (red trace in Supplementary Fig. S1a). Specifically, the gel-filtration profile of the purified EF-Tu (theoretically 46 kDa including the hexahistidine tag) showed three distinct eluates of the monomer (the last eluate with an estimated hydrodynamic size of 45 kDa), dimer (middle, 81 kDa), and high-order oligomer (column void-volume eluate) species. The particle sizes deduced for the first two eluates by dynamic light scattering also supported the presence of a dimeric (81 kDa with a 4-nm radius) and 20-mer oligomeric (883 kDa with an 11-nm radius) species (Supplementary Fig. S1b). In addition, the purified EF-Tu showed a potent tendency of time-dependent aggregation leading to gradual precipitation during a few days of storage at room temperature. Storage at a low temperature (4 °C) for more than 4 days also resulted in nearly complete conversion to the oligomeric state, thereby yielding mostly a single eluate at the column void volume (blue trace in Supplementary Fig. S1a).

In contrast, the gel-filtration result for a different preparation with continuous use of excess Mg^{2+} during all steps of protein expression and purification showed a single species of the elution corresponding to its monomeric size (black trace in Supplementary Fig. S1a), which was maintained during storage at 4 °C for

more than 4 days (gray trace in Supplementary Fig. S1a). However, adding a chelating agent (ethylenediaminetetraacetic acid, or EDTA) to the Mg^{2+}-containing EF-Tu solution resulted in severe precipitation of the protein, which indicated that the Mg^{2+} ion bound to EF-Tu is crucial for the stability of the protein. In addition, the oligomerization of Mg^{2+}-bound EF-Tu also proceeded at elevated temperatures (green trace in Supplementary Fig. S1a) and was accelerated at higher temperatures, indicating its intrinsically thermounstable property.

Reduced form-specific binding of Hsp33 to EF-Tu

A pull-down assay was performed to examine Hsp33 binding to EF-Tu by employing the hexahistidine-tagged monomeric EF-Tu form (^{Mono}EF-Tu) as bait for binding to the Ni^{2+}-affinity resin, along with three Hsp33 preparations at different redox statuses (^{R}Hsp33, ^{hO}Hsp33, and ^{O}Hsp33) as prey. ^{R}Hsp33 was bound to the resin-bound EF-Tu (Fig. 1a), whereas both ^{hO}Hsp33 and ^{O}Hsp33 showed no significant binding (Supplementary Fig. S2a). EF-Tu binding to ^{R}Hsp33 was then examined by NMR spectroscopy (Fig. 1b). The [^{1}H/^{15}N] transverse relaxation optimized spectroscopy (TROSY) spectrum of ^{R}Hsp33 showed significant line broadening upon the addition of ^{Mono}EF-Tu, indicating the formation of a complex with the protein. Subsequently, we attempted to measure the binding affinity using isothermal titration calorimetry (ITC). Consistent with the pull-down assay results, no significant binding of ^{hO}Hsp33 and ^{O}Hsp33 to ^{Mono}EF-Tu was observed (Supplementary Fig. S2b). Unexpectedly, the ITC thermogram for ^{R}Hsp33 binding to ^{Mono}EF-Tu showed an unusual trace characterized by continuous endothermic reactions following exothermic pulses (Fig. 1c). This abnormal thermogram was ultimately explained by the conformational change of EF-Tu after ^{R}Hsp33 binding (see Discussion). However, the exothermic traces with endothermic interference inevitably hindered the ability to conduct a reliable analysis to estimate thermodynamic parameters. Alternatively, we measured ^{R}Hsp33 binding to the preformed oligomeric EF-Tu (^{Oligo}EF-Tu; void-volume fraction as shown in Supplementary Fig. S1a), which permitted a well-fitted estimation (Fig. 1c): K_d of 0.58 ± 0.13 μM ($\Delta H = -78.6 \pm 3.47$ kJ·mol^{-1}; $\Delta G = -35.7$ kJ·mol^{-1}) with a stoichiometry of approximately two ($N = 2.37 \pm 0.06$) ^{R}Hsp33 molecules to one EF-Tu oligomer, using the aforementioned 20-mer oligomeric size (Supplementary Fig. S1b) for EF-Tu. Thus, the chaperone-inactive, reduced form of Hsp33, but not the oxidized forms, was revealed to be relevant to both ^{Mono}EF-Tu and ^{Oligo}EF-Tu binding.

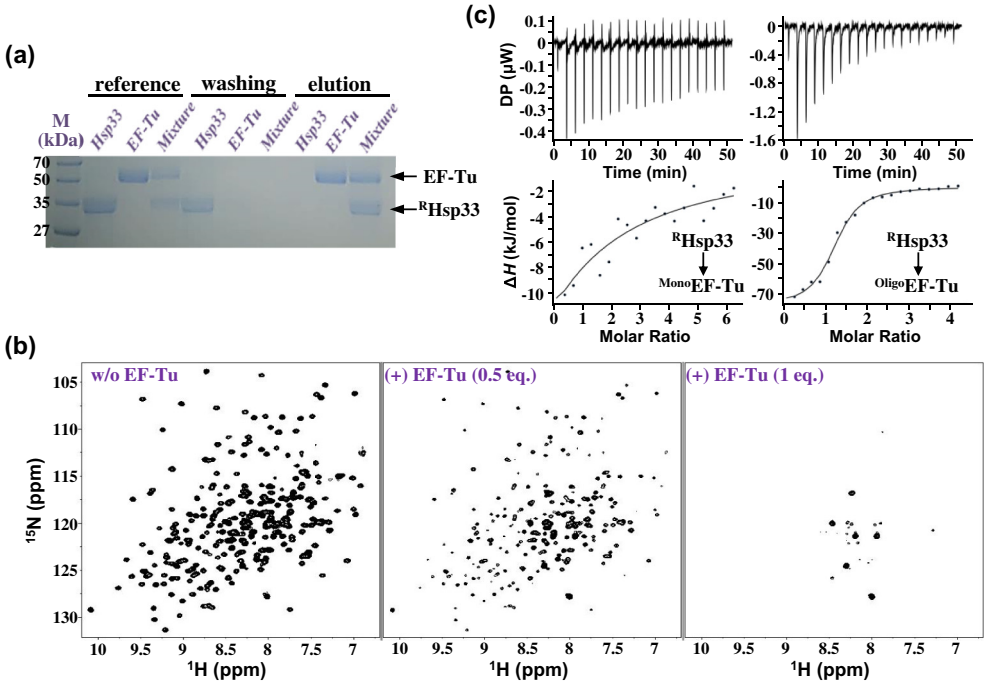

Fig. 1. Molecular interaction between ^{R}Hsp33 and EF-Tu. (a) Pull-down assay using His-tag-fused ^{Mono}EF-Tu as a bait molecule that binds to the resin, while employing ^{R}Hsp33 as a prey molecule. The protein solution was mixed with the resin, followed by washing and subsequent elution. Each solution was resolved by SDS-PAGE (M, size marker). (b) NMR ([^{1}H/^{15}N]TROSY) spectrum of [^{15}N]^{R}Hsp33 (0.3 mM) in the absence (left) and presence of 0.5 (middle) and 1 (right) equimolar EF-Tu. (c) ITC measurement for ^{R}Hsp33 binding to ^{Mono}EF-Tu (left) and ^{Oligo}EF-Tu (right). Each point in the binding isotherm (lower panels) represents the integrated heat of the associated peak in the thermogram (upper panels).

EF-Tu oligomerization and aggregation promoted by ^{R}Hsp33

Considering our NMR instrumental conditions, the quite severe line broadening of the ^{R}Hsp33 NMR spectrum in the presence of ^{mono}EF-Tu was unusual and alluded to the massive complex formation beyond the one-to-one binding of the two proteins. Thus, considering the intrinsic propensity of EF-Tu to oligomerization (Supplementary Fig. S1a), we reasoned that a huge complex system of the two proteins might be created by EF-Tu oligomerization, which was verified by gel-filtration analysis. When the ^{Mono}EF-Tu solution was incubated with ^{R}Hsp33 at 30 °C for 30 min, the gel-filtration profile of the mixture showed three distinct elution peaks commonly containing both proteins (red trace and the corresponding gel electrophoresis image in Fig. 2a). The last elution was attributable to small fractions of non-complexed proteins (note that the hydrodynamic size of ^{R}Hsp33 is comparable with that of ^{Mono}EF-Tu; see green and black traces in Fig. 2a, respectively). The middle elution can be accounted for by the one-to-one complex of the proteins based on the estimated hydrodynamic size of approximately 80 kDa. The largest elution at the column void volume indicated the presence of high-order oligomers of the complex. Longer (1 h) incubation led to appreciable enlargement of the oligomer fraction with a concomitant decrement of monomeric and heterodimeric species (blue trace in Fig. 2a). Furthermore, with longer incubation of the complex, the oligomer size became increasingly enlarged, as reflected by the shortened retention times of oligomer fractions for longer-incubated samples (Fig. 2b). This continuously expanding size implied that the oligomerizing process could eventually result in irreversible aggregation.

Although it was not clear whether EF-Tu, ^{R}Hsp33, or both were responsible, the observed oligomerization/aggregation was more vigorous with a higher concentration of EF-Tu (e.g., compare the relative proportion of the oligomer fraction in blue trace of Fig. 2a, performed with 50 μM of EF-Tu, with that in red trace of Fig. 2b, performed with 15 μM of EF-Tu), as well as at a higher incubation temperature (e.g., compare red trace of Fig. 2b, performed at 30 °C, with black trace of Fig. 2c, performed at approximately 22 °C). Therefore, collectively considering the heat-dependent intrinsic oligomerization of EF-Tu (green in Supplementary Fig. S1a) and the dominant content of EF-Tu in the ^{R}Hsp33:EF-Tu oligomeric fractions (gel electrophoresis images in Fig. 2a), we assumed that ^{R}Hsp33 binding promoted the rapid oligomerization of EF-Tu. We also checked whether the ^{R}Hsp33-mediated oligomerization of EF-Tu was affected by guanine nucleotides (GDP and GTP), whose binding is known to enhance the EF-Tu stability [28]. As expected from the higher affinity of GDP than GTP [29], the oligomerizing efficiency

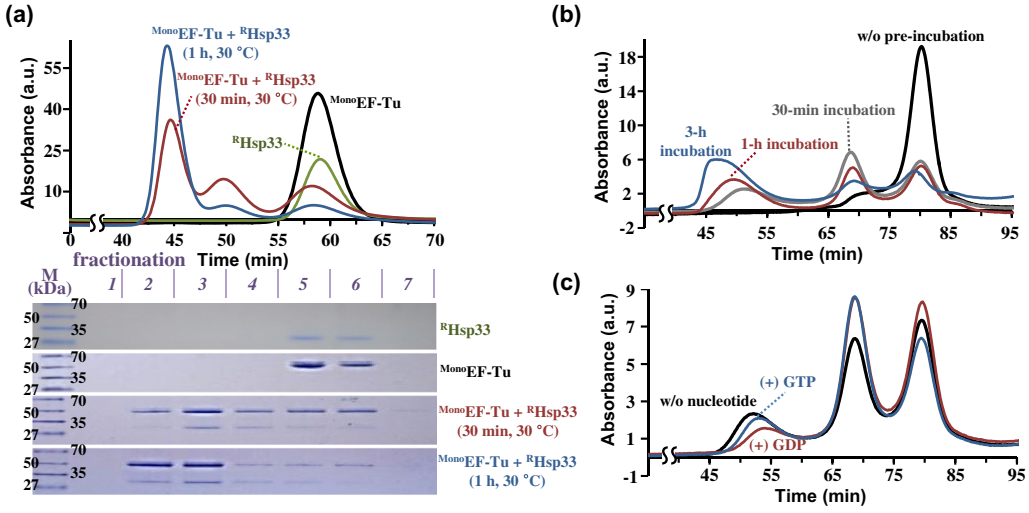

Fig. 2. Promotion of EF-Tu oligomerization by ^{R}Hsp33. The analytical gel-filtration assay was performed at room temperature using a Superdex 75 (a) or Superdex 200 (b and c) column, at a flow rate of 1 mL/min in 50 mM HEPES buffer (pH 7.4) containing 150 mM NaCl, 5 mM $MgSO_4$, 100 μM $ZnSO_4$, and 5 mM DTT. (a) Effect of ^{R}Hsp33. The mixture of ^{Mono}EF-Tu (50 μM) and ^{R}Hsp33 (25 μM) was incubated at 30 °C for 30 min (red) or for 1 h (blue) prior to injection. Standard profiles for isolated ^{R}Hsp33 and ^{Mono}EF-Tu are presented by green and black lines, respectively. All individual eluents were fractionated every 5 min and resolved by 12% Tricine–SDS-PAGE (lower panel; M, molecular size marker). (b) Incubation time-dependent increase of oligomeric size. The ^{Mono}EF-Tu (15 μM) and ^{R}Hsp33 (15 μM) mixture was injected immediately after mixing (black) and after incubation at 30 °C for 30 min (gray), 1 h (red line), or 3 h (blue). (c) Effects of guanidine nucleotides. The equimolar (15 μM) mixture of ^{Mono}EF-Tu and ^{R}Hsp33 without nucleotides (black) or containing 60 μM of GTP (blue) or GDP (red) migrated after 1-h pre-incubation at room temperature (approximately 22 °C). Control profiles in the absence of ^{R}Hsp33 are presented in Supplementary Fig. S3.

(relative proportion of the oligomer fraction and the oligomer size) of EF-Tu was lowest in its GDP-bound state, whereas the nucleotide-free form showed the fastest oligomerization mediated by ^{R}Hsp33 (Fig. 2c and Supplementary Fig. S3). However, none of the nucleotides inhibited Hsp33-mediated EF-Tu oligomerization, demonstrating the outperforming negative influence of ^{R}Hsp33 on EF-Tu stability. Finally, the EF-Tu aggregation was monitored over time by light scattering (Fig. 3). The intrinsic production of ^{Oligo}EF-Tu in the absence of ^{R}Hsp33 (green in Supplementary Fig. S1a) was reflected by the gradual, albeit slight, increase of light scattering, particularly after 20 min of ^{Mono}EF-Tu incubation at 30 °C (red in Fig. 3). The addition of ^{R}Hsp33 promptly accelerated the increase of light scattering (blue in Fig. 3), in support of the vigorous aggregation of EF-Tu.

Oligomer-specific degradation of EF-Tu by Lon protease

As EF-Tu is known to be a substrate of Lon protease in cells [24], the susceptibility of EF-Tu to Lon was compared between ^{Mono}EF-Tu and its intrinsically converted form, ^{Oligo}EF-Tu (Fig. 4a). Notably, ^{Mono}EF-Tu appeared to be resistant to the proteolysis by Lon, whereas ^{Oligo}EF-Tu was efficiently digested. The slight degradation of ^{Mono}EF-Tu detected after a 2-h incubation with Lon was attributable to the small fraction of oligomers created spontaneously during incubation (see green trace in Supplementary Fig. S1a). EF-Tu degradation by Lon was also prominent in the presence of ^{R}Hsp33 (Fig. 4b), implying that the ^{R}Hsp33-induced ^{Oligo}EF-Tu was competent for rapid digestion by Lon. Furthermore, EF-Tu degradation was highly accelerated when its mixture with ^{R}Hsp33 was pre-incubated for efficient oligomerization prior to

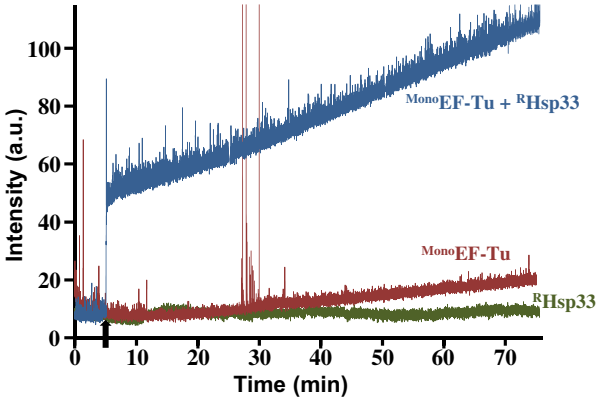

Fig. 3. Real-time monitoring of EF-Tu aggregation. Light (400 nm) scattering of ^{Mono}EF-Tu (100 μM) solution in the absence (red) and presence (blue) of ^{R}Hsp33 (50 μM; added at 5 min of incubation, as indicated by a black arrow) was recorded over the indicated incubation time at 30 °C. The control trace for ^{R}Hsp33 is presented by green line.

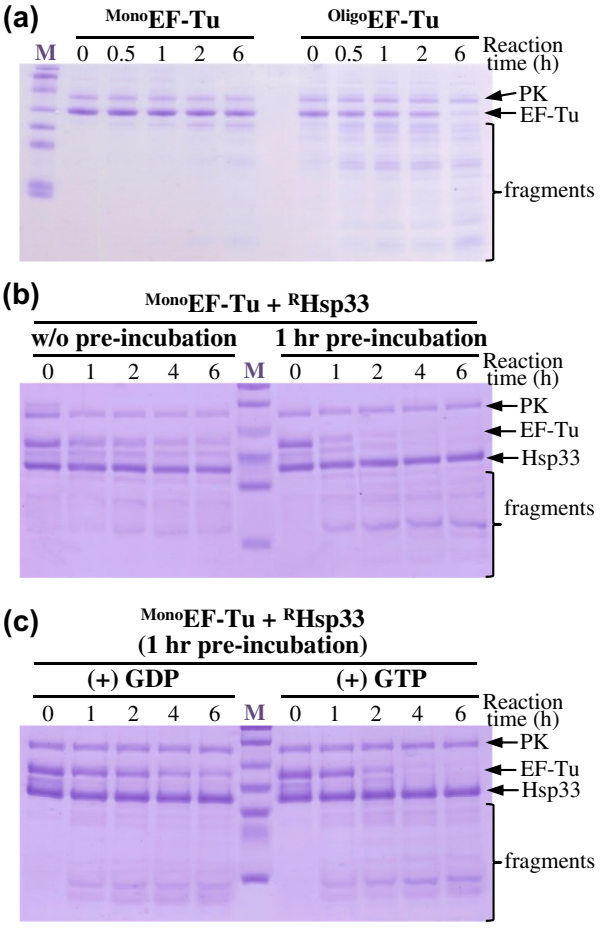

Fig. 4. Specific digestion of oligomeric EF-Tu by Lon protease. EF-Tu (10 μM) reacted at 30 °C with 0.26 nM Lon protease supplemented with pyruvate kinase (PK; 5 μM) for ATP generation and was resolved by SDS-PAGE (12% Tricine gel). The 0-h sample was taken immediately after adding the protease to the reaction mixture. (a) ^{Mono}EF-Tu and ^{Oligo}EF-Tu preparations were subjected as substrates. (b) The equimolar (10 μM) mixture of ^{Mono}EF-Tu and ^{R}Hsp33 reacted with Lon, without or after 1-h pre-incubation. (c) The ^{Mono}EF-Tu and ^{R}Hsp33 mixture containing 40 μM of GTP or GDP was pre-incubated for 1 h, followed by a reaction with Lon.

reaction with Lon (Fig. 4b). Moreover, guanosine nucleotides that slightly suppressed the oligomerization (Fig. 2c) also resulted in marginal retardation of the degradation (Fig. 4c). Together, these results suggest that ^{Oligo}EF-Tu was specifically subjected to Lon proteolysis, and ^{R}Hsp33 binding could facilitate the Lon-mediated EF-Tu degradation by promoting its oligomerization. We further confirmed that Hsp33 could also be susceptible to Lon depending on its unfolding status; that is, the isolated ^{hO}Hsp33 with partial unfolding and ^{O}Hsp33 with extended unfolding [15,20,22] invoked moderate and rapid digestion, respectively (Supplementary Fig. S4). However, ^{R}Hsp33, as well as the pyruvate kinase that was

contained in the reaction mixture for ATP generation, remained intact during EF-Tu degradation (Fig. 4b and c). Hence, a certain conformational event specific to EF-Tu could be anticipated in the ^{R}Hsp33:EF-Tu complex.

Conformational destabilization of EF-Tu catalyzed by ^{R}Hsp33

Structural determinants discriminating the proteolytic competence between ^{Mono}EF-Tu and ^{Oligo}EF-Tu were investigated by spectroscopic experiments. Notably, the far-UV circular dichroism (CD) spectrum of ^{Oligo}EF-Tu, compared with that of ^{Mono}EF-Tu, was characterized by a gain in random-coil and β-sheet contents at the significant expense of α-helical content (Fig. 5a), which is usually described as partial unfolding and aggregation. The minute spectral change of ^{Mono}EF-Tu after 30 min at 30 °C (inset in Fig. 5a) was also attributable to the spontaneous production of a small portion of ^{Oligo}EF-Tu that probably entailed partial unfolding. The fluorescence spectrum of ^{Oligo}EF-Tu-bound 8-anilino-1-naphthalene sulfonic acid (ANS; green in Fig. 5b) showed a markedly higher intensity and a substantial (>25 nm) blue shift compared to the ^{Mono}EF-Tu-bound ANS emission (black in Fig. 5b), indicating a change in the tertiary structure with an expansion of the hydrophobic surfaces.

We next monitored the ^{R}Hsp33-induced conformational change of EF-Tu. The CD spectrum of the ^{R}Hsp33:^{Mono}EF-Tu complex was nearly identical to the theoretical sum of individual protein spectra (compare blue trace and open circles in Fig. 5c), indicating no significant conformational change upon binding. However, subsequent incubation of the mixture resulted in a significant spectral change (red in Fig. 5c; decreased and increased signals at around 220 nm and 200 nm, respectively) indicative of partial unfolding. The unfolding of ^{Mono}EF-Tu alone occurred gradually over incubation time (black in the inset of

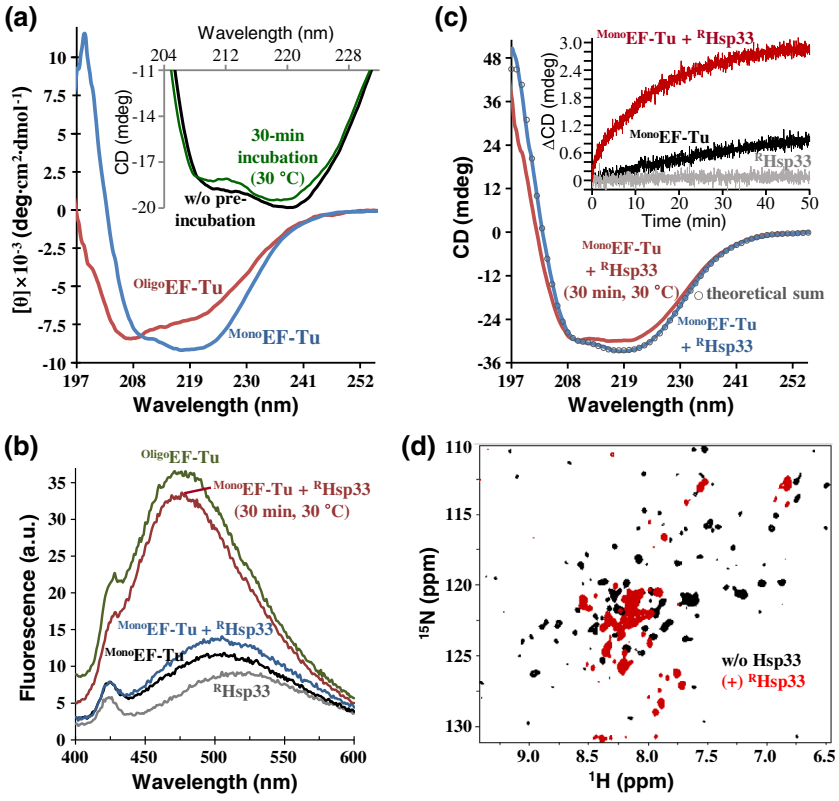

Fig. 5. Conformational change of EF-Tu concomitant to oligomerization. (a) Normalized ([θ], mean residue molar ellipticity) far-UV CD spectra for 8 μM of ^{Mono}EF-Tu (blue) and ^{Oligo}EF-Tu (red). The inset shows an enlarged region of the CD spectra for 5 μM ^{Mono}EF-Tu before (black) and after (green) incubation at 30 °C for 30 min. (b) ANS fluorescence spectra of ^{Mono}EF-Tu (black), ^{Oligo}EF-Tu (green), ^{R}Hsp33 (gray), and an equimolar (5 μM) mixture of ^{Mono}EF-Tu and ^{R}Hsp33 (blue, before incubation; red, after 30-min incubation at 30 °C). (c) Far-UV CD spectra of an equimolar (5 μM) mixture of ^{Mono}EF-Tu and ^{R}Hsp33 immediately after mixing (blue) and after 30 °C incubation for 30 min (red). Open circles depict the theoretical sums of individual spectra of ^{Mono}EF-Tu and ^{R}Hsp33. The inset shows time-dependent CD signal changes (ΔCD) at 220 nm of 15 μM ^{R}Hsp33 (gray), ^{Mono}EF-Tu (black), and their mixture (red). (d) NMR ([^{1}H/^{15}N]TROSY) spectra of [^{15}N]EF-Tu (0.3 mM) in the absence (black) and presence (red) of equimolar ^{R}Hsp33.

Fig. 5c), whereas the ^{R}Hsp33:^{Mono}EF-Tu complex rapidly underwent intense unfolding (red in the inset of Fig. 5c). The ANS fluorescence spectrum of the ^{R}Hsp33:^{Mono}EF-Tu complex (blue in Fig. 5b) also showed a significant blue shift and intensification after 30 min of incubation (red in Fig. 5b). Although Hsp33 undergoes partial unfolding upon oxidation that exposes hydrophobic surfaces [30,31], such Hsp33 unfolding by unexpected oxidation was unlikely under our experimental condition because the isolated ^{R}Hsp33 showed no significant spectral change during incubation (gray in the inset of Fig. 5c). The proteolytic resistance of ^{R}Hsp33 in complex with EF-Tu (Fig. 4b), in contrast to the efficient digestion of $^{hO/O}$Hsp33 by Lon (Supplementary Fig. S4), could also exclude the possibility of Hsp33 unfolding during incubation of the ^{R}Hsp33:^{Mono}EF-Tu complex.

The NMR results provided more convincing evidence for the EF-Tu-specific conformational change. Although the readily precipitating property of EF-Tu at the high concentration for NMR prohibited obtaining a high-quality spectrum, the measured NMR spectrum of ^{Mono}EF-Tu showed many resolved peaks that reflect a well-ordered conformation (black in Fig. 5d). In contrast, the ^{R}Hsp33-titrated EF-Tu spectrum (red in Fig. 5d) showed overall line broadening as observed in the EF-Tu-titrated ^{R}Hsp33 spectrum (Fig. 1b). Furthermore, upon complex formation, chemical shift perturbations that are relevant to unfolding were evident for the remaining resonances of EF-Tu (red in Fig. 5d), whereas ^{R}Hsp33 resonances retained their chemical shifts (Figs. 1b and 6a). Collectively, the spectroscopic analysis revealed that ^{R}Hsp33, without its own conformational change, catalyzed the conformational change of EF-Tu to a misfolded state.

Involvement of the ^{R}Hsp33 RSD in the EF-Tu interaction

Owing to the immense line broadening in the NMR spectrum of the equimolar ^{R}Hsp33:EF-Tu complex (Fig. 1b), the EF-Tu-interacting residues of ^{R}Hsp33 were qualitatively traced in the presence of a small (0.2 equimolar) amount of EF-Tu (Fig. 6a). The spectrum distinguished some representative residues of ^{R}Hsp33 with their corresponding resonances disappearing upon the addition of EF-Tu. Given that these residues are presumably involved in the specific molecular interaction, the EF-Tu-binding sites appeared to be distributed through all three domains of ^{R}Hsp33. However, it was particularly noteworthy that many residues in the RSD, including the zinc-liganding cysteine C265, are involved in the putative EF-Tu-contacting sites, since the zinc-bound RSD fold

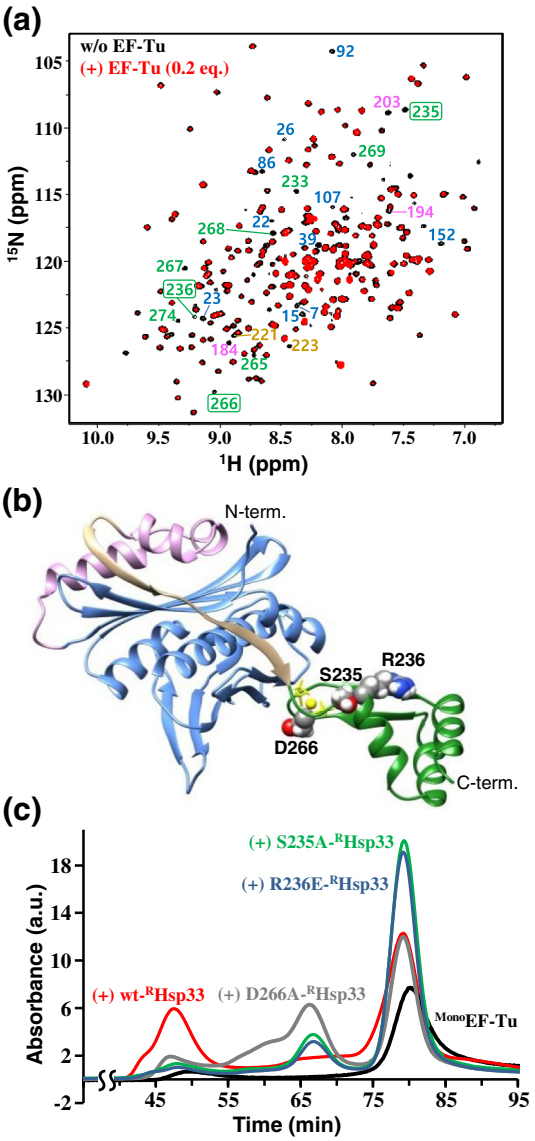

Fig. 6. Critical contribution of the zinc-binding region in ^{R}Hsp33 to EF-Tu binding. (a) NMR ([^{1}H/^{15}N]TROSY) spectra of [^{15}N]^{R}Hsp33 (0.3 mM) at pH 6.5 in the absence (black) and presence (red) of 0.2 equimolar EF-Tu. In the well-resolved regions, indicator peaks (i.e., completely disappearing resonances upon binding) for the NCD, MLD, interdomain linker stretch, and RSD are labeled with corresponding residue numbers colored blue, pink, tan, and green, respectively; those selected for mutagenesis are boxed. (b) Structural description of ^{R}Hsp33. The figure was generated with the atomic coordinates for the semi-empirical model structure of *E. coli* ^{R}Hsp33 determined previously [22]. Color coordinating for each domain follows that in panel a. The bound zinc ion (sphere) and the conserved cysteine side chains (stick models) are depicted in yellow. Sidechains of the S235, R236, and D266 residues for mutagenesis are represented as spheres. (c) Gel-filtration (Superdex 200 column) profiles of ^{Mono}EF-Tu (30 μM; black) and its mixture with equimolar wild-type (red) or a site-directed mutant of ^{R}Hsp33: D266A- (gray), R236E- (blue), or S235A-^{R}Hsp33 (green). All samples contained 40 μM of GDP and were pre-incubated at 30 °C for 1 h before injection.

critically discriminates ^{R}Hsp33 from the EF-Tu binding-defective form, $^{hO/O}$Hsp33. Therefore, among the putative EF-Tu-contacting residues in the RSD, we conducted site-directed mutagenesis for S235, R236, and D266, as these residues are commonly surface-exposed, are adjacent to the zinc-coordinating cysteines C234 and C265 (Fig. 6b), and show a high degree of conservation in Hsp33 orthologs (Supplementary Fig. S5; serine at position 235, a positively charged amino acid at 236, and a polar amino acid at 266): S235A (hydroxyl group removed), R236E (charge reversed), and D266A (charge removed) mutants of ^{R}Hsp33. Compatibility of the RSD to its zinc-bound fold was guaranteed by unaltered CD spectra of the three variants generated (Supplementary Fig. S6). Both the S235A and R236E mutations dramatically impaired the ability of ^{R}Hsp33 to catalyze the EF-Tu oligomerization, while D266A also moderately disrupted the unfoldase/aggregase activity of the protein (Fig. 6c). The considerable defects in aggregating EF-Tu due to directed mutagenesis at these three sites verified that the zinc-binding region of ^{R}Hsp33 critically contributes to its specific binding to EF-Tu.

Binding of the EF-Tu G-domain to the ^{R}Hsp33 RSD

To identify the ^{R}Hsp33 RSD-interacting domains of EF-Tu, we attempted to prepare the following five recombinant proteins corresponding to individual domains of EF-Tu and their deletion variants: G-domain (GD; also referred to as domain-I; residues 1–205), domain-II (D2; residues 204–294), domain-III (D3; residues 294–393), GD-deleted (ΔGD) variant ($^{\Delta GD}$EF-Tu; D2 + D3), and D3-deleted (ΔD3) variant ($^{\Delta D3}$EF-Tu; GD + D2). Among them, D2 and D3 were completely insoluble, while the other proteins, which were moderately soluble, showed relatively poor stability (more rapid precipitation during storage) than intact EF-Tu. Nonetheless, the EF-Tu variant-titrating NMR analysis to monitor some obvious alterations in ^{R}Hsp33 resonances was permitted at different pH values that are relatively more favorable for each EF-Tu variant. As a result, significantly broadened resonances in the EF-Tu GD-titrated ^{R}Hsp33 spectrum (Fig. 7a) were mapped mostly onto the RSD, including the selected mutagenesis positions (S235, R236, and D266). These resonance alterations in the RSD were also well-defined in the $^{\Delta D3}$EF-Tu-titrated spectrum (Fig. 7b), whereas they were not relevant in the $^{\Delta GD}$EF-Tu-titrated spectrum (Fig. 7c). Therefore, the EF-Tu GD was reasonably identified as the specific domain responsible for binding to the RSD of ^{R}Hsp33. The $^{\Delta D3}$EF-Tu (GD + D2)-titrated spectrum, which showed more abundant resonance perturbations than the GD-titrated spectrum, indicated that D2 also contributed to the ^{R}Hsp33 binding of EF-Tu. In addition, the apparently weakened affinity by deleting D3 (compare Fig. 7b for $^{\Delta D3}$EF-Tu with Figs. 1b and 6a for intact EF-

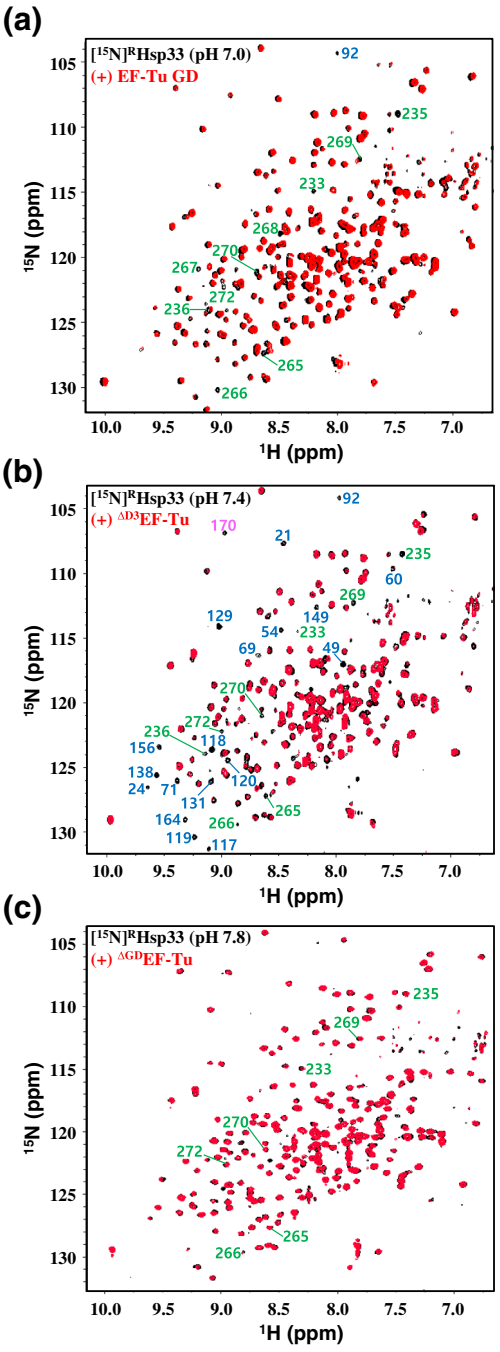

Fig. 7. Binding of the GD in EF-Tu to the zinc-binding region in ^{R}Hsp33. NMR ([^{1}H/^{15}N]TROSY) spectra of [^{15}N]^{R}Hsp33 (0.3 mM) at pH 7.0 (a), 7.4 (b), and 7.8 (c), in the absence (black) and presence (red) of equimolar EF-Tu GD (a), $^{\Delta D3}$EF-Tu (b), and $^{\Delta GD}$EF-Tu (c), are superimposed, respectively. In the well-resolved regions of panel a and b, unambiguous assignments are labeled for significantly affected resonances by the EF-Tu variants (coloring designation follows that described in Fig. 6a).

Tu) implied that D3 in intact EF-Tu was also possibly involved in the ^{R}Hsp33 binding. Collectively, these results suggest cooperative binding of all three domains in intact EF-Tu to accomplish the observed strong binding to ^{R}Hsp33 and/or a subsequent conformational change. However, given the severe defect in ^{R}Hsp33 binding of $^{\Delta GD}$EF-Tu (Fig. 7c), it is also reasonable that the EF-Tu GD binding to the ^{R}Hsp33 RSD could drive the whole molecular interaction of the two proteins. This assumption is in turn strongly underpinned by the previous mutagenesis results (Fig. 6c) that confirmed a critical influence of the mutation at the RSD of ^{R}Hsp33 on its EF-Tu binding capability.

Discussion

This study was conducted to verify a novel function of the molecular chaperone Hsp33, which is potentially associated with the regulation of EF-Tu that is engaged in ribosomal protein synthesis. Originally identified as a redox-regulated holding chaperone, the zinc-bound reduced form of Hsp33 (^{R}Hsp33) has long been regarded as a functionally inactive state that is primed for oxidation-induced activation. In addition, as cellular thermal stress can readily evoke oxidative stress, it is generally considered that overexpression of ^{R}Hsp33 induced by heat represents a rapid response to the oxidative stress following heat stress [14]. However, the present study provides an alternative interpretation that the protein in a reduced state displays its own functionality distinguished from the oxidized form. This ^{R}Hsp33-specific molecular function also appears to be distinct from the reduced form-specific action (i.e., membrane targeting of clients) of the eukaryotic chaperone, Get3, whose redox-regulated molecular system closely resembled that of Hsp33 [4].

The ^{R}Hsp33-specific functionality could be implicit in its well-structured zinc-bound RSD that constitutes a unique fold of the zinc-binding domain [17]. Indeed, the present results demonstrated that the RSD specifically mediated strong (submicromolar K_d) binding of ^{R}Hsp33 to EF-Tu *via* interacting with the GD of EF-Tu. Therefore, the critical involvement of a folded RSD, which is fully unfolded upon oxidation, can explain the defective binding of oxidized Hsp33 to EF-Tu. The RSD-mediated specific binding of ^{R}Hsp33 to EF-Tu also suggests that EF-Tu would be a *bona fide* client of ^{R}Hsp33. Furthermore, the strong binding of ^{R}Hsp33 subsequently evoked the aberrant folding of EF-Tu, which proceeded intensely after ^{R}Hsp33 binding. Therefore, the unusual thermogram of ^{R}Hsp33 binding to ^{Mono}EF-Tu (Fig. 1c) is a result of the unfolding process of EF-Tu, which is generally postulated to be an endothermic reaction, following the likely exothermic binding of ^{R}Hsp33. The EF-Tu unfolding that also exposed hydrophobic surfaces inevitably resulted in its aggressive oligomerization, leading to irreversible aggregation. Therefore, the molecular effect of ^{R}Hsp33 binding can be regarded as efficient downregulation of both the conformational (unfolding) and colloidal (aggregation) stability of EF-Tu. Given the intrinsic unfolding/aggregation of EF-Tu in the absence of Mg^{2+} (Supplementary Fig. S1a), the ^{R}Hsp33-mediated unfolding/aggregation of the Mg^{2+}-bound ^{Mono}EF-Tu may entail the release of bound Mg^{2+} from its GD. However, it was evident that ^{R}Hsp33 could also bind to the Mg^{2+}-free ^{Oligo}EF-Tu (Fig. 1c). In addition, in cells, the Mg^{2+}-free EF-Tu, which is formed by its elongation factor thermal-stable (EF-Ts) binding for GDP-GTP exchange, is stabilized by the bound EF-Ts [26,27]. Unlike the EF-Ts interaction, which occurs through the GD and D3 of EF-Tu [29], GD/D2 or all three domains of EF-Tu appear to cooperatively interact with ^{R}Hsp33 (Fig. 7). Therefore, as the interdomain communication is a critical element of intact EF-Tu stability [28], it is inferred that EF-Tu destabilization by ^{R}Hsp33, irrespective of Mg^{2+} release, might be accomplished by the adverse modulation of the interdomain interaction in EF-Tu.

Conclusively, the present results showed that the specific binding of ^{R}Hsp33 promoted the unfolding/aggregation reaction of the substrate protein, EF-Tu, whereas the bound ^{R}Hsp33 was not subjected to such an alteration. Therefore, although it remains to be further elucidated whether ^{R}Hsp33 actively unfolds EF-Tu or if the ^{R}Hsp33 binding to already unfolding EF-Tu shifts the equilibrium toward the unfolded aggregation-prone state, to our knowledge, this study provides the first example of aggregase activity displayed by a molecular chaperone. In addition, the unfoldase activity of ^{R}Hsp33, which targets the functional native fold of the specific substrate EF-Tu to induce its aberrant folding, is also distinctive from the unfoldase activity of other known molecular chaperones, such as GroEL and AAA+ ring proteases, which act on stable misfolded polypeptides [10–13]. Moreover, the AAA+ ring proteases, including Lon, require ATP for their unfoldase activity, which is coupled with subsequent proteolytic activity [12,13], whereas the unfoldase action of Hsp33 does not consume ATP. In the case of the chaperonin, GroEL, ATP-independent unfoldase activity can be exerted in connection with a subsequent ATP-consuming reaction for client refolding [32], whereas the unfoldase action of ^{R}Hsp33 results in ATP-independent aggregation of the substrate. In this context, Hsp33 can be appreciated as a unique example of an ATP-independent molecular chaperone that can play a distinctive dual function as an unfoldase/aggregase (i.e., ^{R}Hsp33) and as a holding chaperone (i.e., ^{O}Hsp33) depending on the redox status.

In cells, ^{R}Hsp33-bound EF-Tu would lose its functionality for translation elongation as a result of the aberrant conformational change. In addition, given that Lon protease is an essential component of the cellular proteostasis network recognizing and degrading misfolded proteins [12,13], the unfoldase/

aggregase action of ^{R}Hsp33 on EF-Tu in cells would make EF-Tu recognizable by Lon. Although EF-Tu was identified as a *bona fide* substrate of Lon protease in cells [24], our results revealed that the natively folded ^{Mono}EF-Tu is not susceptible to the proteolytic degradation by Lon (Fig. 4a). In contrast, the prominent digestion of spontaneous ^{Oligo}EF-Tu by Lon (Fig. 4a) is attributable to the increased hydrophobic surfaces (Fig. 5b), as the Lon protease preferentially recognizes hydrophobic patches in misfolded proteins [12,13]. Likewise, the aberrant folding and aggregation of the ^{R}Hsp33-bound EF-Tu could be readily recognized by Lon for efficient degradation, whereas bound ^{R}Hsp33 was resistant to proteolysis. Therefore, the EF-Tu-specific degradation by Lon in cells would enable ^{R}Hsp33 to be recycled to further attenuate the translation elongation through the dysregulation of EF-Tu. This plausible process for EF-Tu degradation in cells by the collaborative action of ^{R}Hsp33 and Lon can be harmful to cell growth, unless prevented and/or compensated by another regulatory system. Indeed, Bruel *et al*. [24] observed that the Hsp33 overproduction in a DnaK-deficient *E. coli* strain exhibited strong toxicity to bacterial growth under normal conditions by up-regulating the Lon-mediated degradation of EF-Tu. Conversely, however, growth of the DnaK-deficient cells at non-permissive temperatures was rescued by overexpressing Hsp33 [24], which implies that the EF-Tu degradation by ^{R}Hsp33 and Lon could be beneficial for bacterial survival under stressful conditions. Particularly in heat shock, global pausing of elongation is a widespread cellular translation regulation mechanism for cell survival [33], since heat stress promotes the noxious misfolding and aggregation of proteins synthesized in the ribosome. In this regard, dysregulation of EF-Tu would contribute to the survival of heat-stressed cells by attenuating the translational elongation of otherwise misfolded proteins that are deleterious to cells. Therefore, given the overexpression of ^{R}Hsp33 by heat shock, the present results demonstrating the ^{R}Hsp33-catalyzed degradation of EF-Tu by Lon may implicate ^{R}Hsp33 in the elongation-posing machinery for cell survival in response to thermal stressors, which can also contribute to cellular proteostasis by regulating the proteome-wide turnover rate in cells.

In summary, this study highlighted the unfoldase activity of the molecular chaperone, Hsp33, that catalyzes the structural conversion of EF-Tu to an aggregation- and proteolysis-prone state. This unfoldase/aggregase activity of ^{R}Hsp33, which is contradictory to the holding functionality of ^{O}Hsp33 preventing the client aggregation by pausing the unfolding process, was achieved *via* its specific interaction with the natively folded EF-Tu, in contrast to the sequence non-specific promiscuous interaction of ^{O}Hsp33 with universal unfolding intermediates. In particular, the intriguing kinetics (Fig. 5c) and thermodynamics (Fig. 1c) of EF-Tu unfolding/aggregation upon ^{R}Hsp33 binding suggest that this paradigm could serve as an excellent model system for further in-depth analyses of the protein unfolding and/or misfolding pathway. In addition, it is worth searching for the specific substrates of ^{R}Hsp33 other than EF-Tu to validate the client-specific functionality of ^{R}Hsp33. As a recent proteomics analysis of Hsp33 identified dozens of promising Hsp33-binding partners [34], their molecular interactions with ^{R}Hsp33 and the structural consequences remain to be systematically explored. Considering the fact that Hsp33 is expressed at basal levels even under non-stressed conditions [4], the specific cellular functionality of ^{R}Hsp33 is expected to be increasingly revealed through further studies on the individual molecular interactions of ^{R}Hsp33 with those putative clients.

Materials and Methods

DNA construct and protein preparations

All primer sequences used for subcloning and mutagenesis are summarized in Supplementary Table S1. Recombinant Hsp33 proteins were prepared as described previously [20,22]. Briefly, the pUJ30 (pET11a-*hslO*) plasmid [14] was used as a template for PCR-amplification of the *hslO* (*E. coli* Hsp33) gene and subsequent introduction of single-site mutations. The amplified DNA fragments were then inserted into the pET21a vector between the NdeI and XhoI restriction sites. The reverse primers contained a stop codon to produce the protein without artificial histidine tags. The constructed plasmids were transformed into the *E. coli* strain, JH13 (BL21, Δ*hslO*), [35] for mutants, whereas *E. coli* BL21(DE3)pLysS cells were transformed with the construct for wild-type Hsp33. The protocol for wild-type Hsp33 was followed for the expression and purification of the mutant proteins. Oxidation of the purified protein was performed by incubating at 43 °C for 3 h in the presence of H_2O_2 (2 mM) as an oxidant, followed by separation of the oxidized species [20,22].

For the *E. coli* EF-Tu construct, the corresponding open reading frame was PCR-amplified using the genomic DNA of the *E. coli* BL21(DE3)pLysS strain as a template and subsequently inserted into the pCold-I (Takara) vector between the *Nde*I and *Xho*I restriction sites, thereby adding an N-terminal hexahistidine tag on the expressed protein. The constructed plasmid for wild-type EF-Tu was used as a template for subsequent subcloning of EF-Tu variants. Following verification by DNA sequencing, the recombinant plasmids were transformed into the *E. coli* strain BL21(DE3)pLysS for protein expression. The transformed cells were grown in Luria–Bertani medium at 37 °C until the optical density at 600 nm reached about 0.7, followed by induction of the expression by adding IPTG (1 mM) and $MgSO_4$

(1 mM) at 17 °C for 18 h. Cell lysis buffer contained 50 mM Tris–HCl (pH 7.4), 1 mM dithiothreitol (DTT), 5 mM $MgSO_4$, 70 mM imidazole, and 100 mM NaCl. Protein purification was performed *via* the sequential application of Ni^{2+}-affinity, anion-exchange, and gel-permeation chromatography in the standard buffer containing 1 mM DTT and 5 mM $MgSO_4$. For rapid oligomerization of EF-Tu, residual DTT and magnesium ions were removed from the purified ^{Mono}EF-Tu solution using the PD-10 column (GE Healthcare), followed by treatment of the solution with 1 mM EDTA. ^{Oligo}EF-Tu was then collected from the supernatant of the EDTA-treated solution for subsequent spectroscopic (CD and fluorescence) analyses. The other procedures followed the protocols established for Hsp33.

Analytical gel filtration

Gel filtration was performed on a HiLoad 16/600 Superdex™ 75 or Superdex™ 200 column (GE Healthcare) connected to a fast protein liquid chromatography system at a flow rate of 1 mL/min in 50 mM HEPES buffer (pH 7.4) containing 150 mM NaCl, 5 mM $MgSO_4$, 100 μM $ZnSO_4$, and 5 mM DTT. The injection volume of each analyte was approximately 2 mL, and the eluting proteins were detected by measuring absorbance at 280 nm. The hydrodynamic size of each protein was represented by the apparent molecular mass (kDa), which was deduced from the elution volume [20,22], in comparison with molecular mass standards of the gel filtration calibration kits (GE Healthcare), LMW (for Superdex 75) and HMW (for Superdex 200).

Pull-down assay

Thirty microliters of Ni^{2+}-charged His-Bind Agarose Resin suspension (ELPisBio, Korea) pre-equilibrated in a standard buffer [50 mM HEPES (pH 7.4), 50 mM NaCl, 5 mM $MgSO_4$, 100 μM $ZnSO_4$, and 1.3 mM β-mercaptoethanol] was mixed with the bait protein (hexahistidine-tagged EF-Tu) solution in the same buffer to a final volume of 100 μL and a final bait concentration of 30 μM, followed by 4 °C incubation for 15 min. After three washes (repeated adding buffer and spin down of resin) with the standard buffer containing 70 mM imidazole, 100 μL of prey solution (60 μM ^{R}Hsp33) was added to the bait-bound resin, followed by end-over-end mixing and subsequent 1-h incubation at 4 °C. The resin suspension was then washed three times with 100 μL of standard buffer containing 70 mM imidazole and 0.4% (v/v) NP-40. Bound materials were then eluted with 100 μL of standard buffer containing 600 mM imidazole. After spin-down removal of the resin, the supernatant (eluted solution) was resolved by sodium dodecyl sulfate-polyacrylamide gel electrophoresis (SDS-PAGE). When the oxidized species of Hsp33 (80 μM of ^{hO}Hsp33 or ^{O}Hsp33) was examined as prey, $ZnSO_4$ and β-mercaptoethanol were excluded in all buffer solutions used.

Lon-proteolysis assay

One hundred microliters of substrate protein (EF-Tu and/or Hsp33) solution (10 μM) in 20 mM sodium phosphate buffer (pH 7.4) containing 50 mM NaCl, 100 μM $MgSO_4$, 50 μM $ZnSO_4$, 100 μM ATP, and 5 μM pyruvate kinase (Merck) was reacted with 0.26 nM of recombinant *E. coli* Lon protease (Sino Biological) at 30 °C. To halt the Lon reaction, 1 μL of EDTA stock (100 mM) and 5 μL of Protease Inhibitor Cocktail (Merck) stock (1 mg/mL) solution were added into every sample (10 μL) taken at designated sampling times, followed by boiling with SDS-PAGE sample buffer (10 μL) and subsequent storage in a deep freezer until use for the SDS-PAGE run. When the oxidized species of Hsp33 (^{hO}Hsp33 or ^{O}Hsp33) was examined as substrate, $ZnSO_4$ was excluded in all buffer solutions used.

Light scattering analysis

The ^{Oligo}EF-Tu (100 μM) solution in 50 mM HEPES buffer (pH 7.4) containing 150 mM NaCl and 5 mM DTT was thoroughly filtered using a membrane filter (Advantec) with a pore diameter of 0.2 μm. Dynamic light scattering data of the solution were collected on a Viscotek 802 dynamic light scattering instrument (Malvern Instruments), followed by the molecular weight determination using OmniSIZE software (Malvern Instruments). The aggregation of ^{Mono}EF-Tu (100 μM) at 30 °C in the absence and presence of half-equimolar ^{R}Hsp33 was monitored by recording the kinetic traces of light scattering from the protein solution at 400 nm (5-nm slit width for both excitation and emission), using a Varian Cary Eclipse spectrofluorophotometer with continuous stirring. The solvent buffer (pH 7.4) contained 50 mM HEPES, 50 mM NaCl, 5 mM $MgSO_4$, 100 μM $ZnSO_4$, and 5 mM DTT.

ITC analysis

Binding thermodynamics were measured at 25 °C using a MicroCal Auto-iTC200 calorimeter. ^{Mono}EF-Tu (70 μM) solutions in 50 mM HEPES buffer (pH 7.4) containing 50 mM NaCl, 5 mM $MgSO_4$, 50 μM $ZnSO_4$, and 5 mM DTT were contained in the reaction cell (200 μL), whereas ^{R}Hsp33 (210 μM) solutions in the same buffer were titrated from the syringe (40 μL). When ^{Oligo}EF-Tu was contained in the reaction cell, $MgSO_4$ was excluded in all buffer solutions used. A titration experiment consisted of 20 injections: 0.4 μL of the first injection followed by 19 injections (2 μL each) with an injection interval of 150 s. The obtained thermogram was analyzed by data fitting on a single-site binding model, using

a commercial software package (ORIGIN 7.0) provided by the manufacturer. When the oxidized species of Hsp33 (^{hO}Hsp33 or ^{O}Hsp33) was titrated, $ZnSO_4$ and DTT were excluded in all buffer solutions used.

CD spectroscopy

A 0.1-cm path length cell was used for the CD measurements of individual protein samples (5–20 μM) dissolved in 15 mM sodium phosphate buffer (pH 7.4) containing 15 mM NaCl, 20 μM $ZnSO_4$, and 20 μM $MgSO_4$. For this buffer condition, the ^{mono}EF-Tu stock solution that contained 5 mM $MgSO_4$ was buffer-exchanged to 1 mM $MgSO_4$, followed by dilution to the designated concentration (20 μM $MgSO_4$) before measurement. Standard far-UV CD spectra were recorded on a Jasco J-710 spectropolarimeter at room temperature (approximately 22 °C) with a 1-nm bandwidth and a 1-s response time. Three individual scans taken from 260 to 190 nm with a 0.1- or a 1-nm step resolution were summed and averaged, followed by subtraction of blank buffer CD signals. Time-course CD changes were monitored at 220 nm at 30 °C using an Applied Photophysics Chirascan CD spectrometer equipped with a temperature controller. The signals were recorded at every 0.1 s with a 1-nm bandwidth.

Fluorescence spectroscopy

Protein solutions (5 μM) containing no or 11 μM of the fluorescent probe ANS (Merck) were prepared in 50 mM HEPES buffer (pH 7.4) containing 50 mM NaCl, 5 mM DTT, 5 mM $MgSO_4$, and 100 μM $ZnSO_4$. Fluorescence spectra were recorded in a Varian Cary Eclipse spectrofluorophotometer at 30 °C with continuous stirring. The excitation wavelength was fixed at 370 nm (slit width 1 nm), while fluorescence emissions were scanned from 400 to 600 nm (slit width 1 nm).

NMR spectroscopy

The isotope-[^{15}N]-enriched proteins for NMR measurements were produced by culturing the protein-expressing cells in M9 minimal medium supplemented with $^{15}NH_4Cl$ as the sole nitrogen source. NMR samples contained 0.3 mM of the [^{15}N]-labeled target protein and varying concentrations of its interacting non-labeled counterpart, dissolved in 50 mM HEPES buffer (pH 7.4) containing 50 mM NaCl, 5 mM $MgSO_4$, 1 mM $ZnSO_4$, 5 mM DTT, and 7% (v/v) D_2O. Conventional [^{1}H/^{15}N]TROSY spectra were measured at 298 K on a Bruker Biospin Avance 900 spectrometer equipped with a cryoprobe. The previously assigned chemical shift values [22] were used for residue-specific analysis of the ^{R}Hsp33 spectra.

Acknowledgments

This work was supported by the National Research Foundation (Grant Nos. 2010-0006022, 2013R1A1A2007774, and 2016R1A2B4009700) funded by the Korean government (MEST). We thank Dr. U. Jakob (University of Michigan, USA) for generously providing the recombinant plasmid pUJ30 and the *E. coli* strain JH13. The use of NMR, CD, fluorescence, and ITC equipment was supported by the Korea Basic Science Institute (Ochang, Korea) under the R&D program (Project No. D37700) supervised by the Ministry of Science and ICT.

Appendix A. Supplementary data

Supplementary data to this article can be found online at https://doi.org/10.1016/j.jmb.2019.02.022.

Received 19 December 2018;
Received in revised form 12 February 2019;
Accepted 18 February 2019
Available online 27 February 2019

Keywords:
proteostasis;
protein quality control;
protein turnover;
protein misfolding;
protein aggregation

†K.-S. Jo was supported by Basic Science Research Program through the National Research Foundation of Korea (NRF) funded by the Ministry of Education (grant no. G201809G00019).

Present address: Y.-S. Lee, Analytics Team, R&D Division, POLUS Inc., Incheon 21984, Republic of Korea.

Abbreviations used:
ANS, 8-anilino-1-naphthalene sulfonic acid; CD, circular dichroism; D2, domain-II; D3, domain-III; DTT, dithiothreitol; EDTA, ethylenediaminetetraacetic acid; EF-Ts, elongation factor thermal-stable; EF-Tu, elongation factor thermal-unstable; GD, guanidine nucleotide-binding domain; Hsp33, heat shock protein 33; ITC, isothermal titration calorimetry; MLD, middle linker domain; RSD, redox-switch domain; TROSY, transverse relaxation optimized spectroscopy.

References

[1] E.A. Craig, J.S. Weissman, A.L. Horwich, Heat shock proteins and molecular chaperones: mediators of protein conformation and turnover in the cell, Cell 78 (1994) 365–372.

[2] D. Balchin, M. Hayer-Hartl, F.U. Hartl, In vivo aspects of protein folding and quality control, Science 353 (2016) aac4354.
[3] S. Bershtein, W. Mu, A.W.R. Serohijos, J. Zhou, E.I. Shakhnovich, Protein quality control acts on folding intermediates to shape the effects of mutaions on organismal fitness, Mol. Cell 49 (2013) 133–144.
[4] J.-U. Dahl, M.J. Gray, U. Jakob, Protein quality control under oxidative stress conditions, J. Mol. Biol. 427 (2015) 1549–1563.
[5] S.M. Doyle, O. Genest, S. Wickner, Protein rescue from aggregates by powerful molecular chaperone, Nat. Rev. Mol. Cell Biol. 14 (2013) 617–629.
[6] F.U. Hartl, A. Bracher, M. Hayer-Hartl, Molecular chaperones in protein folding and proteostasis, Nature 475 (2011) 324–332.
[7] C.L. Klaips, G.G. Jayaraj, F.U. Hartl, Pathways of cellular proteostasis in aging and disease, J. Cell Biol. 217 (2017) 51–63.
[8] M. Taipale, G. Tucker, J. Peng, I. Krykbaeva, Z.Y. Lin, B. Larsen, et al., A quantitative chaperone interaction network reveals the architecture of cellular protein homeostasis pathways, Cell 158 (2014) 434–448.
[9] M. Visscher, S. De Henau, M.H.E. Wildschut, R.M. van Es, I. Dhondt, H. Michels, et al., Proteome-wide changes in protein turnover rates in *C. elegans* models of longevity and age-related disease, Cell Rep. 16 (2016) 3041–3051.
[10] R.U.H. Mattoo, P. Goloubinoff, Molecular chaperones are nanomachines that catalyticallyt unfold misfolded and alternatively folded proteins, Cell. Mol. Life Sci. 71 (2014) 3311–3325.
[11] S. Priya, S.K. Sharma, P. Goloubinoff, Molecular chaperones as enzymes that catalytically unfold misfolded polypeptides, FEBS Lett. 587 (2013) 1981–1987.
[12] L. Van Melderen, A. Aertsen, Regulation and quality control by Lon-dependent proteolysis, Res. Microbiol. 160 (2009) 645–651.
[13] E.F. Vieux, M.L. Wohlever, J.Z. Chen, R.T. Sauer, T.A. Baker, Distinct quaternary structures of the AAA+ Lon protease control substrate degradation, Proc. Natl. Acad. Sci. U. S. A. 110 (2013) E2002–E2008.
[14] U. Jakob, W. Muse, M. Eser, J.C.A. Bardwell, Chaperone activity with a redox switch, Cell 96 (1999) 341–352.
[15] M. Ilbert, J. Horst, S. Ahrens, J. Winter, P.C.F. Graf, H. Lilie, et al., The redox-switch domain of Hsp33 functions as dual stress sensor, Nat. Struct. Mol. Biol. 14 (2007) 556–563.
[16] J. Winter, M. Ilbert, P.C. Graf, D. Ozcelik, U. Jakob, Bleach activates a redox-regulated chaperone by oxidative protein unfolding, Cell 135 (2008) 691–701.
[17] H.-S. Won, L.Y. Low, R. De Guzman, M. Martinez-Yamout, U. Jakob, H.J. Dyson, The zinc-dependent redox switch domain of the chaperone Hsp33 has a novel fold, J. Mol. Biol. 341 (2004) 893–899.
[18] B. Groitl, S. Horowitz, K.A. Makepeace, E.V. Petrotchenko, C.H. Borchers, D. Reichmann, et al., Protein unfolding as a switch from self-recognition to high-affinity client binding, Nat. Commun. 7 (2016), 10357.
[19] D. Reichmann, Y. Xu, C.M. Cremers, M. Ilbert, R. Mittelman, M.C. Fitzgerald, et al., Order out of disorder: working cycle of an intrinsically unfolded chaperone, Cell 148 (2012) 947–957.
[20] Y.-S. Lee, K.-S. Ryu, S.-J. Kim, H.-S. Ko, D.-W. Sim, Y.-H. Jeon, et al., Verification of the interdomain contact site in the inactive monomer, and the domain-swapped fold in the active dimer of Hsp33 in solution, FEBS Lett. 586 (2012) 411–415.
[21] C.M. Cremers, D. Reichmann, J. Hausmann, M. Ilbert, U. Jakob, Unfolding of metastable linker region is at the core of Hsp33 activation as a redox-regulated chaperone, J. Biol. Chem. 285 (2010) 11243–11251.
[22] Y.-S. Lee, J. Lee, K.-S. Ryu, Y. Lee, T.-G. Jung, J.-H. Jang, et al., Semi-empirical structure determination of *Escherichia coli* Hsp33 and identification of dynamic regulatory elements for the activation process, J. Mol. Biol. 427 (2015) 3850–3861.
[23] W.-Y. Wholey, U. Jakob, Hsp33 confers bleach resistance by protecting elongation factor Tu against oxidative degradation in *Vibrio cholerae*, Mol. Microbiol. 83 (2012) 981–991.
[24] N. Bruel, M.P. Castanié-Cornet, A.M. Cirinesi, G. Koningstein, C. Georgopoulos, J. Luirink, et al., Hsp33 controls elongation factor-Tu stability and allows *Escherichia coli* growth in the absence of the major DnaK and trigger factor chaperones, J. Biol. Chem. 287 (2012) 44435–44446.
[25] W. Voth, U. Jakob, Stress-activated chaperones: a first line of defense, Trends Biochem. Sci. 42 (2017) 899–913.
[26] C. Maracci, M.V. Rodnina, Translational GTPases, Biopolymers 105 (2016) 463–475.
[27] C.G. Noble, H. Song, Structural studies of elongation and release factors, Cell. Mol. Life Sci. 65 (2008) 1335–1346.
[28] H. Šanderová, M. Hůlková, P. Maloň, M. Kepková, J. Jonák, Thermostability of multidomain proteins: elongation factors EF-Tu from *Escherichia coli* and *Bacillus stearothermophilus* and their chimeric forms, Protein Sci. 13 (2004) 89–99.
[29] S.S. Thirup, L.B. Van, T.K. Nielsen, C.R. Knudsen, Structural outline of the detailed mechanism for elongation factor Ts-mediated guanine nucleotide exchange on elongation factor Tu, J. Struct. Biol. 191 (2015) 10–21.
[30] P.C.F. Graf, M. Martinez-Yamout, S. VanHaerents, H. Lilie, H.J. Dyson, U. Jakob, Activation of the redox-regulated chaperone Hsp33 by domain unfolding, J. Biol. Chem. 279 (2004) 20529–20538.
[31] L.V.S. Raman, T. Kumar, C.M. Rao Ramakrishna, Redox-regulated chaperone function and conformational changes of *Escherichia coli* Hsp33, FEBS Lett. 489 (2001) 19–24.
[32] S. Priya, S.K. Sharma, V. Sood, R.U. Mattoo, A. Finka, A. Azem, et al., GroEL and CCT are catalytic unfoldases mediating out-of-cage polypeptide refolding without ATP, Proc. Natl. Acad. Sci. U. S. A. 110 (2013) 7199–7204.
[33] R. Shalgi, J.A. Hurt, I. Krykbaeva, M. Taipale, S. Lindquist, C. B. Burge, Widespread regulation of translation by elongation pausing in heat shock, Mol. Cell 49 (2013) 439–452.
[34] S. Rimon, O. Suss, M. Goldenberg, R. Fassler, O. Yogev, H. Amartely, et al., A role of metastable regions and their connectivity in the inactivation of a redox-regulated chaperone and its inter-chaperone crosstalk, Antioxid. Redox Signal. 27 (2017) 1252–1267.
[35] J. Graumann, H. Lilie, X. Tang, K.A. Tucker, J.H. Hoffmann, J. Vijayalakshmi, et al., Activation of the redox-regulated molecular chaperone Hsp33—a two-step mechanism, Structure 9 (2001) 377–387.